EXPERIMENTAL AND THEORETICAL ANALYSIS OF N,N'-(ETHANE-1,2-DIYLBIS(4,1-PHENYLENE)) BIS(1-(THIOPHEN-2-YL)METHANIMINE) AND N,N'-(ETHANE-1,2-DIYLBIS(4,1-PHENYLENE))BIS(1-(4-METHYLTHIOPHEN-2-YL)METHANIMINE) SCHIFF BASE LIGANDS

GUHERGUL ULUCAM[a] AND BUSRA YENTURK[a]*

Department of Chemistry, Faculty of Sciences, Trakya University, Edirne, Turkey.

A BSTRACT

N,N'-(ethane-1,2-diylbis(4,1-phenylene))bis(1-(thiophen-2-yl)methanimine) and N,N'-(ethane-1,2-diylbis(4,1-phenylene))bis(1-(4-methylthiophen-2-yl) methanimine) ligands are formed by diamine and two aromatic aldehyde using Schiff base condensation method. Ligands are characterised by fourier transform infrared spectroscopy (FT-IR), ^{1}H- and ^{13}C- nuclear magnetic resonance spectroscopy (^{1}H- and ^{13}C- NMR) and mass spectroscopy (LC ESI/MS) methods. Furthermore, geometric properties such as bond lenghts, bond angles, dihedral angles, electronic properties, highest occupied molecular orbital (HOMO) and lowest unoccupied molecular orbital (LUMO) energies are calculated by using Gaussian 09w program. Experimental and theoretical spectrum datas are compared.

Keywords: thiophene, schiff base, Gaussian 09w, DFT/B3LYP.

1. INTRODUCTION

There are many studies investigating the anti-inflammatory, anticancer, analgesic, antioxidant and antimicrobial effects of Schiff base ligands.[1-5] These ligands and their metal complexes have many application fields such as coordination chemistry, industry, pharmacology, medicine, chemical and biological processes since they have donor atoms such as O, N, S.[6-10] Bibenzyl of isoquinoline alkaloids is an important component of some drugs, and widely used in the synthesis of products such as synthetic agents and opioid analgesics as pointed out elsewhere.[11,12]

Examination of the theoretical properties of the ligands has recently attracted the attention of scientists. These methods help identify physical, geometric, electronic and optical properties that give information about the molecule.[13-19] Therefore, theoretical and experimental studies have gained importance especially for chemists.

The aim of this study was to investigate the synthesis and theoretical properties of Schiff base ligands derived from bibenzyl. The ligands were synthesized by Schiff base condensation method [8,9] of thiophene-2-carbaldehyde and 4-methylthiophene-2-carbaldehyde with 4,4'-(ethane-1,2-diyl)dianiline, respectively. Ligand 1 has been synthesized in a slightly different way than our study, but its physical geometrical, optical and electronic properties have not been calculated.[12] Ligand 2 synthesis was not found in the literature. The obtained ligand structures were explained by Fourier transform infrared spectroscopy (FT-IR), ^{1}H- and ^{13}C- nuclear magnetic resonance spectroscopy (^{1}H- and ^{13}C-NMR) and mass spectroscopy (LC ESI/MS). The theoretical properties of Schiff base ligands were investigated using B3LYP/6-311G++(2d,p) basis sets and density functional theory (DFT). NMR and FT-IR spectra were calculated by using Gaussian G09w program package.[20] The bond lenghts, the bond angles, the dihedral angles, the molecular electrostatic potential map (MEP), the dipol moments, the highest occupied molecular orbital (HOMO) and the lowest unoccupied molecular orbital (LUMO) of ligands were found.

2. MATERIALS AND METHODS

2.1. Material

Perkin-Elmer BXII spectrometer in 450-4000cm^{-1} range was used for FT-IR spectrum. ^{1}H- and ^{13}C-NMR spectrums were taken by using Varian 300MHz and Varian 75.5MHz deuterated chloroform (CDCl$_3$) solvents, respectively. Mass spectra were acquired with Agilent Technologies 6460 Triple Quad LC ESI/MS.

2.2. Synthesis of Schiff Base Ligands

4,4'-(ethane-1,2-diyl)dianiline (1.06g, 5mmol) and thiophene-2-carbaldehyde (1.12g, 10mmol) were dissolved in two separate flasks containing 50ml of methanol. Then, two solutions were mixed for one hour. At this time, 1-2 drops of glacial acetic acid were added to the mixture. Reaction was continued for two days with applied heating. Methanol, which is used as a solvent, was then removed by rotary evaporator. The residual viscous material was dried in vacuum oven after kept in hexane: chlorofom (20:10ml) for a period of time. The dark yellow powder solid was synthesized with N,N'-(ethane-1,2-diylbis(4,1-phenylene))bis(1-(thiophen-2-yl)methanimine), 1.22 grams and %60 yield.[8,21] Melting point is found as 146 ^{o}C. Synthesis procedure was repeated with 4,4'-(ethane-1,2-diyl)dianiline and 4-methylthiophene-2-carbaldehyde (1.2g, 10mmol) as an aldehyde, based on the same stoichometric ratios. The second dark yellow powder solid was synthesized with N,N'-(ethane-1,2-diylbis(4,1-phenylene))bis(1-(4-methylthiophen-2-yl)methanimine), 1.66 grams and %81 yield. Melting point is found as 163 ^{o}C. The formation of **(1)** and **(2)** ligands is shown in Figure 1.

(1): FT-IR (cm^{-1}): 3074-2875, 1631, 1515, 745. **^{1}H NMR (300MHz, CDCl3, δ, ppm):** 2.95 (2H, CH2), 7.11-7.26 (5H, m, CH), 7.50 (2H, d, CH), 8.58 (1H, s, CHN). **^{13}C NMR (75.5MHz, CDCl3, δ, ppm):** 37.74 (CH2), 121.23, 127.97, 127.97, 129.51, 129.51, 130.51, 132.26, 139.87, 143.19, 149.35, 154.32. **ESI/MS (m/z)** [M+H]$^{+}$, (401.0000).

(2): FT-IR (cm^{-1}): 3021-2854, 1614, 1548, 750. **^{1}H NMR (300MHz, CDCl3, δ, ppm):** 2.25-2.31 (2H, CH2), 2.93 (3H, CH3), 7.33-7.10 (6H, m, CH), 8.50 (1H, s, CHN). **^{13}C NMR (75,5MHz, CDCl3, δ, ppm):** 15.9 (CH3), 37.74 (CH2), 121.16, 121.16, 126.15, 126.15, 127.97, 129.35, 134.34, 138.34, 142.72, 149.50, 152.70. **ESI/MS (m/z)** [M+H]$^{+}$, (429.0000).

2.3. Theoretical Method

In Gaussian G09w program package[20], calculations were made by 6-311++G(2d,p) basis set using B3LYP theory with Becke's three parameter hybrid variable function and Lee-Yang-Parr's correlation function.[22-26] NMR and FT-IR spectrums were calculated from optimized geometrics using the same method and basis set. GIAO method was used in theoretical ^{1}H- and ^{13}C-NMR chemicals shift formations. FT-IR spectrum was corrected multiplying by 0.9613 in order to fix theoretial errors.[22,25,27] Bond lengths, bond angles, dihedral angles, HOMO-LUMO energies are calculated for **(1)** and **(2)** ligands by usind DFT and 6-311++G(2d,p) basis set. Also, molecular electrostatik potential map (MEP) was shown. The theoretical spectroscopic data of molecule was compared with experimental data.

3. RESULTS AND DISCUSSIONS

3.1. Molecular Geometry

Three dimension of the **(1)** and **(2)** ligands geometry with minimized energy was plotted in GaussView. These geometries are shown in Figure 2 to reflect cross sectional view of the symmetrical ligand arms. In these molecular structures, H protons were represented by the numbers of the C atoms to which they are bound in the spectrum data but not shown except the methyl hydrogens in the **(2)** ligand.

C2-C1-C1'-C2' dihedral angle, which determines the shape of the both ligands, is determined to be 68.3º for **(1)** ligand and 67.5º for **(2)** ligand where it provides the ligands to be tapered as V-shaped. The bond lenghts between the atoms of the ligands are given in Table I and important bond angles and dihedral angles are given in Table II. Since the ligands have a symmmetrical structure around the diphenylethane bridge the datas of a particular part of this symmetry are included in the tables.

e-mail: gulergul@trakya.edu.tr

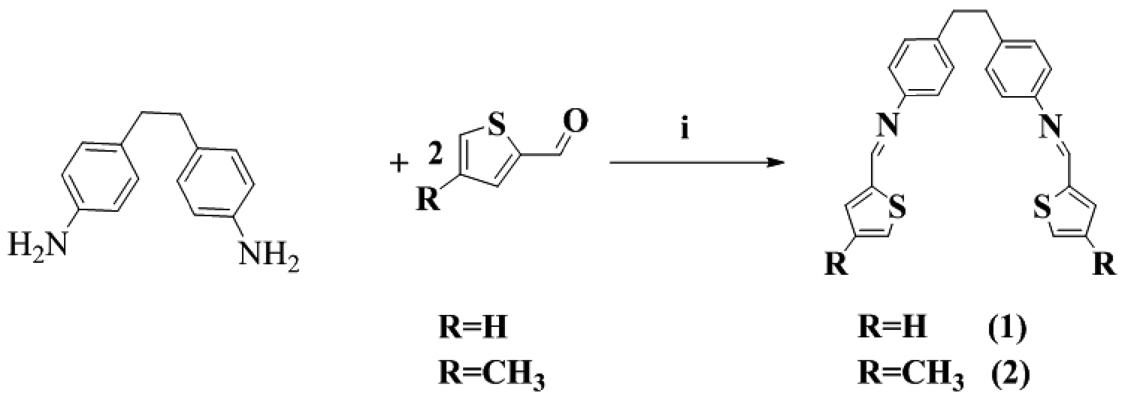

Fig. 1. Reaction of ligands of **(1)** and **(2)** (i: methanol, glacial acetic acid).

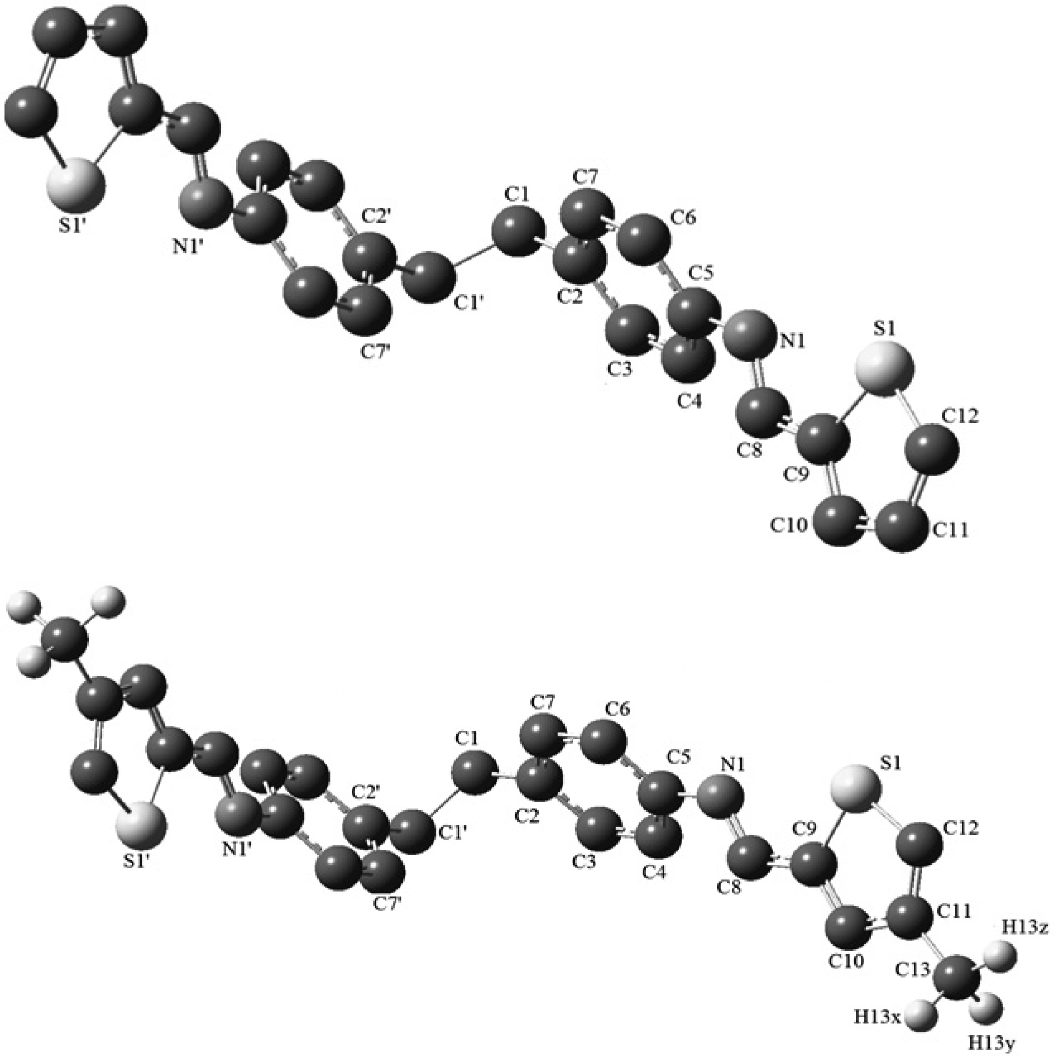

Fig. 2. Molecular configuration of ligands **(1)** and **(2)** (top: **(1),** bottom: **(2)**)

Table I. Theoretical bond lengths of ligands **(1)** and **(2).**

Bond lengths (Å)	**(1)**	**(2)**
C1-C2	1.509	1.509
C1-H1x	1.093	1.093
C1-H1y	1.094	1.094
C2-C7	1.397	1.396
C7-C6	1.387	1.387
C6-C5	1.398	1.398
C5-C3	1.401	1.401
C3-C2	1.388	1.388
C5-C6	1.397	1.397
C5-N1	1.403	1.403
N1-C8	1.276	1.276
C8-C9	1.443	1.443
C9-C10	1.375	1.374
C10-C11	1.416	1.422
C11-C12	1.367	1.369
C12-S1	1.725	1.727
S1-C9	1.742	1.741
C8-H8	1.097	1.097
C11-C13	-	1.502
C13-H13x	-	1.093
C13-H13y	-	1.093
C13-H13z	-	1.090

Table II. Theoretical bond angles and dihedral angles of ligands **(1)** and **(2).**

Bond angles (˚)	**(1)**	**(2)**	Dihedral angles (˚)	**(1)**	**(2)**
C1-C2-C7	121.59	121.56	C7-C6-C5-N1	179.81	179.82
C2-C7-C6	121.33	121.36	C6-C5-N1-C8	145.17	144.67
C7-C6-C5	120.65	120.63	C5-N1-C8-C9	177.34	177.28
C3-C5-N1	123.56	123.51	N1-C8-C9-S1	-1.185	-1.297
C5-N1-C8	120.49	120.43	N1-C8-C9-C10	178.79	178.73
N1-C8-C9	122.75	122.82	C8-C9-C10-C11	-179.91	-179.91
C8-C9-S1	122.27	122.40	C9-C10-C11-C12	-0.0182	-0.0259
C9-S1-C12	91.23	90.91	C10-C11-C12-S1	-0.0389	-0.0232
S1-C12-C11	112.34	113.25	C9-C10-C11-C13	-	179.93
C12-C11-C10	112.29	110.98	C2-C1-C1’-C2’	68.3	67.5
C11-C10-C9	113.26	114.02			
C12-C11-C13	-	124.86			

Bond lenghts, bond angles and dihedral angles of **(1)** and **(2)** ligands are very compatible with each other. The methyl molecules at the ends of the **(2)** ligand are more than **(1)** ligand have no compelling differences between the geometric parameters of the two ligands according to theoretical calculations.

3.2. HOMO-LUMO Analysis and Electronical Properties

Frontier molecular orbitals (FMO) play a major role in determining the electonic and optical properties of a molecule. Energy difference between highest occupied molecular orbital (HOMO) and lowest unoccupied molecular orbital (LUMO) tells us a lot about the molecule. HOMO’s energy is about *Ionization Potantial* (IP) while LUMO’s energy is about *Electron Affinity* (EA).[28] The less energy difference between these two molecular orbitals results with the more polarized molecule. Polarizing molecules are called soft molecules. When energy difference is high, it is said that molecule is hard, meaning the ability to react is low.[17] The energy difference of the HUMO-LOMO molecular orbitals of (**1**) and **(2)** ligands, which are calculated by using B3LYP theory and 6-311++G(2d,p) basis set, is shown in Figure 3. Since the Gaussian output values were from atomic unit (a.u.), these values were converted to electostatic units (1a.u. = 27.2116 eV).[19]

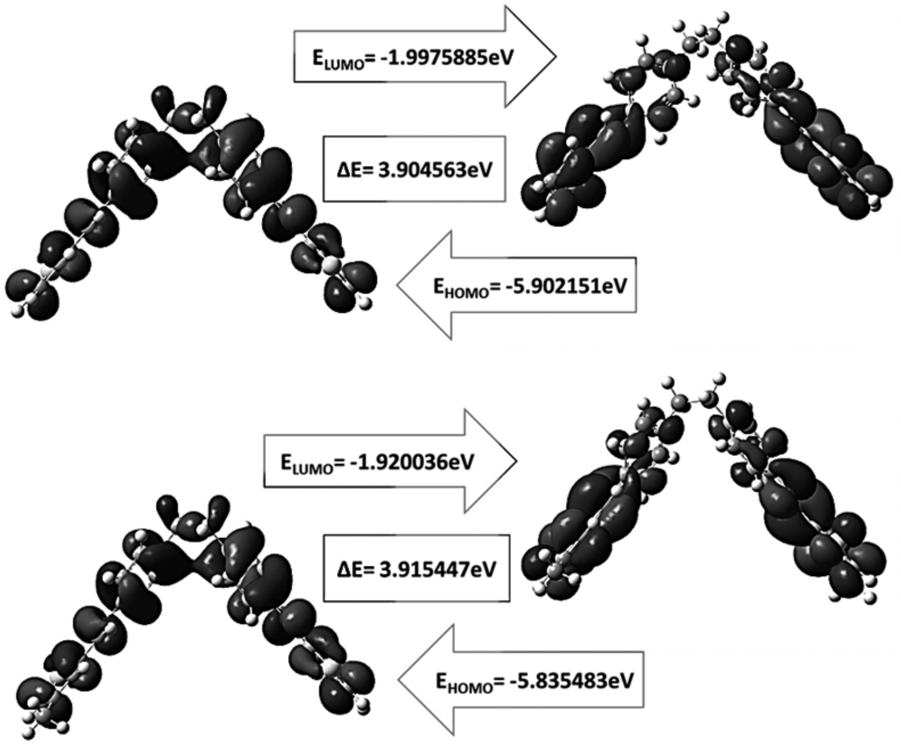

Fig. 3. Energy levels and the 3D plots of the HOMO and LUMO of the title compound at the B3LYP/6-311++(2d,p) level (top: **(1)**, bottom: **(2)**)

Also, electronegativity, chemical potential, chemical hardness and chemical softness were calculated from FMO energies.[19,29,30] Molecular electrical properties are shown in Table III using HOMO and LUMO molecular orbital energies.

Table III. Electronic structure values of ligands **(1)** and **(2).**

	(1)	(2)
E_{HOMO}(eV)	-5.9021517	-5.8354838
E_{LUMO}(eV)	-1.9975885	-1.9200361
$\Delta E = E_{LUMO} - E_{HOMO}$(eV)	3.9094612	3.9154477
IP(eV)	5.9021517	5.8354838
EA (eV)	1.9975885	1.9200361
χ (eV)	3.9498701	3.8777599
φ (eV)	-3.9498701	-3.8777599
η (eV)	1.9522816	1.9577238
σ (eV^{-1})	0.5122218	0.5107972

IP= Ionization Potantial = -HOMO, EA= Electron Affinity = -LUMO,
χ= Electronegativity = (IP+EA)/2, φ = Chemical potential = - χ,
η= Chemical hardness = (IP-EA)/2, σ = Chemical softness = 1/η

3.3. Molecular Electrostatic Potential Surface

Molecular electrostatic potential map (MEP) helps to show positive and negative sites of ligands. This cloud like map provides a qualitative examination of the reactive sites in a ligand. On the map, the red regions refer to the electron rich regions (partial negative charge), and the blue regions refers to the electron poor regions (partial positive charge). In addition, while the regions with fewer electrons are indicated in yellow, almost neutral regions (zero potential) are indicated in green.[30]

MEP map of the ligands is calculated. As shown in Figure 4, the region of the imine group nitrogen is red and the region of sulfur in the five rings is yellow. This red region is electron rich region and might be identified as nucleophilic region. The green areas covering a large part of the ligands concide with the region o the benzene ring and are the region of interest for nucleophiles.

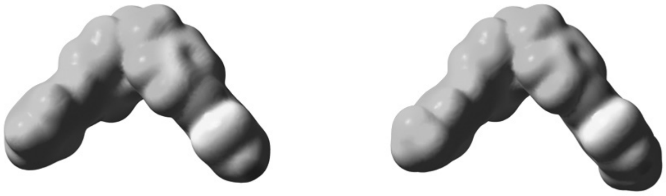

Fig. 4. Molecular electrostatic potential map of ligands **(1)** and **(2)**

3.4. Experimental and Theoretical ¹³C-NMR and ¹H-NMR Chemical Shift Values

According to the ^{13}C-NMR spectrum of the ligand **(1)**, CH_2 carbon was observed at 37.74ppm, while aromatic carbons were observed at 121.23, 127.97, 127.97, 129.51, 129.51, 130.51, 132.26, 139.87, 149.35 and 154.32ppm and CHN carbon at 143.19 ppm. According to the ^{13}C-NMR spectrum of the ligand **(2)**, the CH_3 carbon was observed at 15.90ppm, the CH_2 carbon at 37.74ppm, the aromatic carbons at 121.16, 121.16, 126.15, 126.15, 128.35, 129.35, 134.34, 138.34, 149.50 and 152.70ppm and CHN carbon at 142.72ppm**.**

According to the ^{1}H-NMR spectrum of the ligand **(1)**, CH_2 peak was found at 2.95ppm, aromatic hydrogens peaks were found at 7.11-7.26 and 7.50ppm and the peak of CHN at 8.58ppm. According to the ^{1}H-NMR spectrum of the **(2)** ligand, CH_3 peak was found at 2.25ppm and the CH_2 peak was at 2.93ppm, aromatic component peaks at 7.10-7.33ppm and CHN peak was found a 8.50ppm. According to the experimentally observed chemical shift values for the ligands **(1)** and **(2)** , the proton integrations in the ^{1}H-NMR spectrum were equal to the proton integration in the synthesized structure and the number of carbon in the ^{13}C-NMR spectrum was also appropriate **.**

Table IV. Experimental and theoretical ^{13}C-NMR chemical shift values of ligands **(1)** and **(2)** according to TMS δ / ppm (symmetrical carbons are given in brackets)

	(1)			**(2)**	
Carbon Number	Theoretical	Experimental	Carbon Number	Theoretical	Experimental
C9(C9’)	157.014	154.32	C9(C9’)	157.091	152.70
C5(C5’)	156.614	149.35	C5(C5’)	156.866	149.50
C8(C8’)	153.833	143.19	C8(C8’)	154.412	142.72
C2(C2’)	145.036	139.87	C2(C2’)	145.143	138.34
C12(C12’)	139.669	132.26	C11(C11’)	142.737	134.34
C10(C10’)	135.601	130.51	C10(C10’)	139.025	129.35
C3(C3’)	133.433	129.51	C12(C12’)	135.686	128.35
C7(C7’)	133.258	129.51	C7(C7’)	134.613	126.15
C6(C6’)	130.481	127.97	C3(C3’)	133.755	126.15
C4(C4’)	129.725	127.97	C6(C6’)	129.934	121.16
C11(C11’)	119.300	121.23	C4(C4’)	129.701	121.16
C1(C1’)	43.800	37.74	C1(C1’)	42.785	37.74
			C13(C13’)	16.051	15.90
TMS: tetra methyl silane					

^{13}C-NMR and ^{1}H-NMR chemical shift values for the ligands **(1)** and **(2)** were calculated using the 6-311++G(2d,p) method in the gas phase (Tables IV and V). for the ligand **(1)**, C1(C1’) carbon at 43,800ppm, C8(C8’) carbon at 153,833ppm, C9(C9’), C5(C5’), C2(C2’), C12(C12’), C10(C10’), C3(C3’), C7(C7’), C6(C6’), C4(C4’), C11(C11’) carbons were calculated as 157.014, 156.614, 145.036, 139.669, 135.601, 133.433, 133.258, 130.481, 129.725, 119.300ppm respectively. for the ligand **(2),** C13(C13’) carbon at 16.051ppm, C1(C1’) carbon at 42.785ppm, C8(C8’) carbon at 154.412ppm, C9(C9’), C5(C5’), C2(C2’), C11(C11’), C10(C10’), C12(C12’), C7(C7’), C3(C3’), C6(C6’), C4(C4’) carbons were calculated as 157.091, 156.866, 145.143, 142.737, 139.025, 135.686, 134.613, 133.755, 129.934, 129.701ppm respectively.

In the **(1)** ligand, the C11 carbon had a value of 119.300ppm and in the **(2)** ligand, the C11 carbon had shifted to 142.737ppm because methyl was bound to the same carbon.

For the ligand **(1)**, H1x(H1y’), H1y(H1x’) proton at 2.538, 3.191ppm, H7(H7’), H11(H11’), H6(H6’), H4(H4’), H10(H10’), H3(H3’), H12(H12’) protons, respectively at 6.693, 7.126, 7.186, 7.251, 7.428, 7.479, 7.547ppm, H8(H8’) proton was calculated at 8.658ppm. For the ligand **(2)**, H13z(H13z’), H13y(H13y’), H13x(H13x’) proton at 2.097, 2.165, 2.309ppm, H1x(H1y’), H1y(H1x’) proton at 2.557, 3.133ppm, H7(H7’), H12(H12’), H6(H6’), H4(H4’), H10(H10’), H3(H3’) protons at 6.651, 7.166, 7.191, 7.194, 7.310, 7.492ppm, H8(H8’) proton was calculated at 8.523ppm. It was observed to be appropriate when experimental and theoretical NMR spectrums are compared.

Table V. The experimental and theoretical ^{1}H-NMR chemical shift values of the ligands **(1)** and **(2)** according to TMS **δ** / ppm (symmetrical protons are given in brackets.)

	(1)			**(2)**	
Hydrogen Number	Theoretical	Experimental	Hydrogen Number	Theoretical	Experimental
H8(H8’)	8.658	8.58	H8(H8’)	8.523	8.50
H12(H12’)	7.547	7.50	H3(H3’)	7.492	7.33-7.10
H3(H3’)	7.479		H10(H10’)	7.310	
H10(H10’)	7.428	7.26-7.11	H4(H4’)	7.194	
H4(H4’)	7.251		H6(H6’)	7.191	
H6(H6’)	7.186		H12(H12’)	7.166	
H11(H11’)	7.126		H7(H7’)	6.651	
H7(H7’)	6.693		H1y(H1x’)	3.133	2.93
			H1x(H1y’)	2.557	
H1y(H1x’)	3.191	2.95	H13x(H13x’)	2.309	2.25
H1x(H1y’)	2.538		H13y(H13y’)	2.165	
			H13z(H13z’)	2.097	
TMS: tetra methyl silane					

3.5. Experimental and Theoretical Vibration Frequencies, Spectrums

According to the received FT-IR spectrum, for the ligands **(1)** and **(2)** respectively; All ν(CH) vibrations in the range of 3074-2875 and 3021-2854cm^{-1},[8] ν(C=N) vibration in 1631 and 1614cm^{-1} [31] ν(C=C) aromatic vibration in 1515 and 1548cm^{-1} [31] and the thiophene ring ν(CS) vibration was observed in the vibration 745 and 750cm^{-1}.[8,21,32] It was observed that the primary amines of the starting materials at ~ 3500-3300cm $^{-1}$ had a typical symmetrical and asymmetric ν(NH) and the vibrations of ~ 1750 cm $^{-1}$ de ν(C=O) belonging to the aldehyde were lost.

Vibration frequencies of the ligands **(1)** and **(2)** were calculated using the B3LYP theory and 6-311++G(2d,p) basis set. As it is known, small deviations between vibration frequencies calculated in quantum chemical methods such as DFT level an experimental vibration frequencies are observed. These deviations are derived from the non-harmonic and band overlap effects in experimental measurements.[33] In order to eliminate this deviation, theoretically calculated frequencies were multiplied by 0.9613, which is the appropriate scale factor for the 6-311++G(2d,p) basis set. Selected vibration frequencies of the ligands are presented in Table VI. For the ligand **(1)**, the vibrations ν(C8N1), ν(C12S1) and ν(C9S1) were calculated as 1632, 747 and 667cm^{-1}, respectively. For the ligand **(2)**, the vibrations ν(C8N1), ν(C12S1) and ν(C9S1) were calculated as 1605, 818 and 670cm^{-1}, respectively. It was observed to be appropriate when all the theoretical and experimental vibrations are compared.

Table VI. Experimental and theoretical FT-IR values of ligands **(1)** and **(2)** (cm^{-1}).

(1)				**(2)**			
Selected vib. fre.	Exp. (cm^{-1})	Theo. (cm^{-1})	Selected vib. fre.	Selected vib. fre.	Exp. (cm^{-1})	Theo. (cm^{-1})	Selected vib. fre.
νCH	3074 -2875	3143	νC12H12	νCH	3021-2854	3102	νC12H12
		3109	ν_{s}C12H12 ν_{s}C10H10			3063	ν_{s}C6H6 ν_{s}C7H7
		3094	ν_{as}C11H11 ν_{as}C10H10			3059	νC10H10
		3089	ν_{s}C7H7 ν_{s}C6H6			3052	ν_{s}C4H4 ν_{s}C3H3
		3078	ν_{as}C4H4 ν_{as}C3H3			3041	ν_{as}C6H6 ν_{as}C7H7
		3067	ν_{as}C7H7 ν_{as}C6H6			3024	ν_{as}C4H4 ν_{as}C3H3
						2999	νC13H13
		2980	ν_{as}C1H1xH1y			2950	ν_{as}C1 H1xH1y
		2935	ν_{s}C1H1xH1y			2908	ν_{s}C1H1xH1y
						2906	ν_{s}C13H13xH13yH13z
		2915	νC8H8			2891	νC8H8
νCN	1631	1632	νC8N1	νCN	1614	1605	νC8N1
νCC	1515	1589	νC7C6 νC4C3	νCC	1548	1568	νC7C6 νC4C3
		1552	νC5C4 νC7C2			1536	νC5C4 νC7C2
		1521	νC9C10 νC11C12			1528	νC9C10 νC11C12
δCH		1482	δC4H4 δC3H3 δC7H7 δC6H6			1479	δC4H4 δC3H3 δC7H7 δC6H6
				*m*CH3		1443	*m*C13H13xH13y
*m*CH2		1429	*m*C1H1xH1y	*m*CH2		1431	*m*C1H1xH1y
νCC		1428	νC11C12 νC9C10	νCC		1415	νC11C12 νC9C10
δCH		1356	δC8H8	δCH		1345	δC8H8
γCH2		1311	γC1H1xH1y	γCH2		1321	γC1H1xH1y
γCH		945	γC8H8	γCH		951	γC17H41
νCS	745	747	νC12S1	νCS	750	818	νC12S1
		667	νC9S1			670	νC9S1
Vibration modes: ν_{s}:symmetric streching, ν_{as}:asymmetric streching, δ:rocking, γ:wagging, *m*:scissoring, *b*:twisting. Selected vibration frequencies: Selected vib. fre. Experimental: Exp. Theoretical: Theo.							

4. CONCLUSIONS

The ligands **(1)** and **(2)** were obtained by the Schiff base condensation method of the diamine and the aromatic aldehyde (thiophene-2-carbaldehyde and 4-methylthiophene-2-carbaldehyde, respectively) (Figure 1). The structure of the obtained ligands was described by FT-IR, ^{1}H-NMR, ^{13}C-NMR and LC ESI/MS. The theoretical properties of Schiff base ligands were determined in the gas phase using B3LYP/6-311G++(2d,p) basis set as the bond lengths, the bond angles and the dihedral angles. In addition, NMR and FT-IR values were calculated. It is observed that the theoretical molecular configurations are consistent with those of the experimental findings. By comparing experimental and theoretical spectral data, information about how the molecule is found in space is revealed. The electronegativity, the chemical potential, the chemical softness and the chemical hardness of the ligands were also calculated using theoretically obtained HOMO and LUMO molecular orbital energy values. It is determined from the MEP map that the ligands would show nucleophilic behavior in the regions where their nitrogens are.

ACKNOWLEDGEMENT

The authors acknowledge financial support from Research Fund of Trakya University with the project TÜBAP-2016/22.

5. REFERENCES

1. C. Chandramouli, M. R. Shivanand, T. B. Nayanbhai, B. Bheemachari, R.H. Udupi, *J Chem Pharm Res*, **4**, 1151, (2012)
2. R.P. Chinnasamy, R. Sundararajan, S. Govindaraj, *J Adv Pharm Technol Res*, **1**, 342, (2010)
3. R. Miri, N. Razzaghi-asl, M.K. Mohammadi, *Journal of molecular modeling*, **19**, 727, (2013)
4. P. Venkatesh, *Asian J Pharm Health Sci*, **1**, 8, (2011)
5. D. Wei, N. Li, G. Lu, K. Yao, **49**, 225, (2006)
6. A. Pui, T. Malutan, L. Tataru, C. Malutan, D. Humelnicu, G. Carja, *Polyhedron*, **30**, 2127, (2011)
7. D.M. Boghaei, S. Mohebi, *Tetrahedron*, **58**, 5357, (2002)
8. S. Mihai, M. Negoiu, A. Bondarev, *Rev. Chım. (Bucuresti)*, **60**, 778, (2009)
9. A. Yaul, G. Pethe, R. Deshmukh, A. Aswar, *J. Therm. Anal. Calorim.*, **113**, 745, (2013)
10. J.R. Zamian, E.R. Dockal, *Tran. MetalChem.*, **21**, 370, (1996)
11. R.A. Smith, S. Natelson, **53**, 3476, (1931)
12. R.G. Ramsinghani, Z.A. Filmwala, *WJPPS*, **6**, 1255, (2017)
13. I. Alkorta, J.J. Perez, *Int. J. Quantum Chem.*, **57**, 123, (1996)
14. C. James, C. Ravikumar, T. Sundius, V. Krishnakumar, R. Kesavamoorthy, V.S. Jayakumar, I. Hubert Joe, *Vib. Spectrosc.* , **47**, 10, (2008)
15. D.F.V. Lewis, H.B. Broughton, *ScientificWorldJournal.*, **27**, 1776, (2002)
16. J.S. Murray, K. Sen (1996) Molecular Electrostatic Potentials, Concepts and Applications. 1 edn. Elsevier Science, Amsterdam-Netherlands
17. R.G. Pearson, *Proc. Natl. Acad. Sci. U. S. A.*, **83**, 8440, (1986)
18. J. Šponer, P. Hobza, *Int. J. Quantum. Chem.*, **57**, 959, (1996)
19. A. Vela, J.L. Gazquez, *Am. Chem. Soc.*, **112**, 1490, (1990)
20. M.J. Frisch, G.W. Trucks, H.B. Schlegel, G.E. Scuseria, M.A. Robb, J.R. Cheeseman, G. Scalmani, V. Barone, B. Mennucci, G.A. Petersson, H. Nakatsuji, M. Caricato, X. Li, H.P. Hratchian, A.F. Izmaylov, J. Bloino, G. Zheng, J.L. Sonnenberg, M. Hada, M. Ehara, K. Toyota, R. Fukuda, J. Hasegawa, M. Ishida, T. Nakajima, Y. Honda, O. Kitao, H. Nakai, T. Vreven, J.A. Montgomery, J.E. Peralta, F. Ogliaro, M. Bearpark, J.J. Heyd, E. Brothers, K.N. Kudin, V.N. Staroverov, R. Kobayashi, J. Normand, K. Raghavachari, A. Rendell, J.C. Burant, S.S. Iyengar, J. Tomasi, M. Cossi, N. Rega, J.M. Millam, M. Klene, J.E. Knox, J.B. Cross, V. Bakken, C. Adamo, J. Jaramillo, R. Gomperts, R.E. Stratmann, O. Yazyev, A.J. Austin, R. Cammi, C. Pomelli, J.W. Ochterski, R.L. Martin, K. Morokuma, V.G. Zakrzewski, G.A. Voth, P. Salvador, J.J. Dannenberg, S. Dapprich, A.D. Daniels, Farkas, J.B. Foresman, J.V. Ortiz, J. Cioslowski, D.J. Fox (2009) Gaussian 09, Revision B.01. Wallingford CT.
21. L. Casella, J.A. Ibers, *Inorg. Chem.*, **20**, 2438, (1981)
22. J.B. Foresman, A.E. Frisch (1996) Exploring chemistry with electronic structure methods. 2 edn. Gaussian, Inc, Wallingford, CT
23. J.S. Sreedasyam, J. Sunkari, S. Kundha, R.R. Gundapaneni, *Acta Crystallogr. E.* , **69**, o673, (2013)
24. M. Turkyilmaz, G. Uluçam, Ş. Aktaş, S.E. Okan, *J. Mol. Struct.*, **1136**, 263, (2017)
25. G. Uluçam, S.E. Okan, Ş. Aktaş, G.P. Öğretmen, *J. Mol. Struct.*, **1102**, 146, (2015)
26. G. Ulucam, M. Turkyilmaz, *Bioinorg. Chem. Appl.* , **2018**, 12, (2018)
27. J.S. Al-Otaibi, R.I. Al-Wabli, *Spectrochim. Acta. A Mol. Biomol. Spectrosc.* , **137**, 7, (2015)
28. Ö. Tamer, D. Avcı, Y. Atalay, *J. Phys. Chem. Solids*, **99**, 124, (2016)
29. S. Altürk, D. Avcı, Ö. Tamer, Y. Atalay, *J. Mol. Struct.*, **1164**, 28, (2018)
30. S. Altürk, Ö. Tamer, D. Avcı, Y. Atalay, *J. Organomet. Chem.*, **797**, 110, (2015)
31. M.T. Gabr, N.S. El-Gohary, E.R. El-Bendary, M.M. El-Kerdawy, N. Ni, M.I. Shaaban, *Chin. Chem. Lett.*, **26**, 1522, (2015)
32. K.B. Gudasi, R.S. Vadavi, R.V. Shenoy, S.A. Patil, M. Nethaji, *Trans. Metal. Chem.*, **31**, 374, (2006)
33. M.N. Hriday, R.K. Srivastava, V. Narayan, S. Chand, A.K. Sachan, V.K. Shukla, O. Prasad, L. Sinha, *Res. J. Recent Sci.* , **2**, 150, (2013)